



Delayed Mode QA/QC

Best Practice Manual

Version 1.0

November 2018

Version	Date	Comments	Author
1.0	15/10/2018	Creation of document	Mun Woo

Contents

1	Introduction.....	4
2	Background.....	5
2.1	Gliders and sensor types	5
2.2	Known issues with sensors.....	6
2.2.1	Sea-Bird CTD recorder	6
2.2.2	Examples of Slocum CTD data problems seen in ANFOG data.....	7
2.2.3	Aanderaa Optode	9
2.2.4	Examples of Optode data problems seen in ANFOG Slocum data	12
2.2.5	Bio-optical Sensors	14
2.2.6	Examples of bio-optical data problems seen in ANFOG Slocum data.....	15
3	Delayed-mode QA/QC.....	17
3.1	Glider data and metadata format	17
3.2	Automated data corrections	18
3.2.1	CTD corrections	18
3.2.1.1	Temperature alignment.....	19
3.2.1.2	Thermal lag correction	20
3.2.1.3	Conductivity alignment.....	21
3.2.2	Oxygen Optode corrections.....	23
3.2.2.1	Geometrical alignment.....	24
3.2.2.2	Time lag correction.....	25
3.2.3	Bio-optical data corrections	28
4	Automatic Quality Tests	29
4.1	Impossible date test	29
4.2	Impossible location test.....	29
4.3	Range test.....	30
4.4	Spike test	31
4.5	Gradient test.....	32
4.6	Surface data.....	33
4.7	Descending IRRAD profiles	33
5	Manual Corrections	34
6	QC Report	34
	Bibliography.....	35

1 Introduction

This document is the Australian National Facility for Ocean Gliders (ANFOG) Best Practice manual for ANFOG delayed mode processed data. ANFOG is a facility under Australia's Integrated Marine Observing System (IMOS). ANFOG, with IMOS/ National Collaborative Research Infrastructure Strategy (NCRIS)/ Super Science Initiative (SSI) funding, currently deploys a fleet of 11 gliders all around Australia, successfully completing an average of 30 glider missions annually. The data retrieved from the glider fleet contributes to the study of the major boundary current systems surrounding Australia and their links to coastal ecosystem processes.

This document describes the quality analyses/quality control (QA/QC) methods and correction procedures employed by ANFOG for delayed mode glider data files available for public download through the Australian Ocean Data Network (AODN) portal (<https://portal.aodn.org.au/>) (Figure 1).

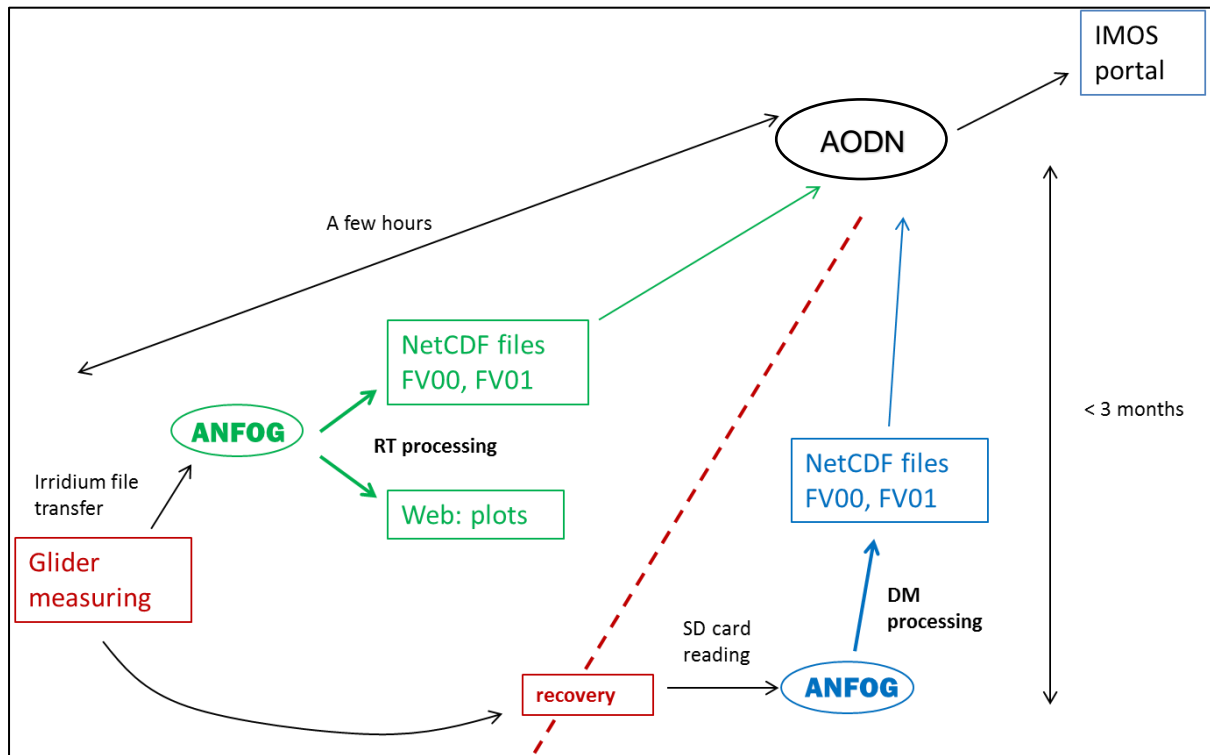


Figure 1 ANFOG data flow chart. AODN stands for Australian Ocean Data Network (an IMOS supported facility), RT for ‘Real Time’ and DM for ‘Delayed Mode’.

2 Background

2.1 Gliders and sensor types

The ANFOG glider fleet consists of two vehicle types: Slocum gliders and Seagliders. Slocum gliders (named for Joshua Slocum the first solo global circumnavigator), manufactured by Teledyne Webb Research Corp, are optimised for shallow coastal waters (< 200 m) where high manoeuvrability is needed. ANFOG currently has 7 Slocum gliders for deployment on the continental shelf. Slocum gliders have an endurance of ~20 days and range of 1,500 km. The Slocum glider first records its position and time stamp at the surface and then performs multiple dive-ascent cycles continuously in a saw-tooth pattern through the water column (Figure 2). After that, it surfaces again to transmit a sample of data, receive new instructions from the base station (if any), and finally it records its position and time stamp before diving into the next segment of saw-tooth sampling. ANFOG gliders are usually configured to sample up to 200 m depth. Currently, all ANFOG Slocum gliders are instrumented with a Seabird-CTD, WETLabs FLBB3 parameters optical sensor (measuring Chlorophyll-a, CDOM and Backscatter), an Aanderaa Oxygen Optode and a Satlantic 4-channel OCR (Ocean Colour Radiometer) downwelling irradiance sensor. Note that Slocum gliders of G1 type used in the past were not equipped with any irradiance sensor.

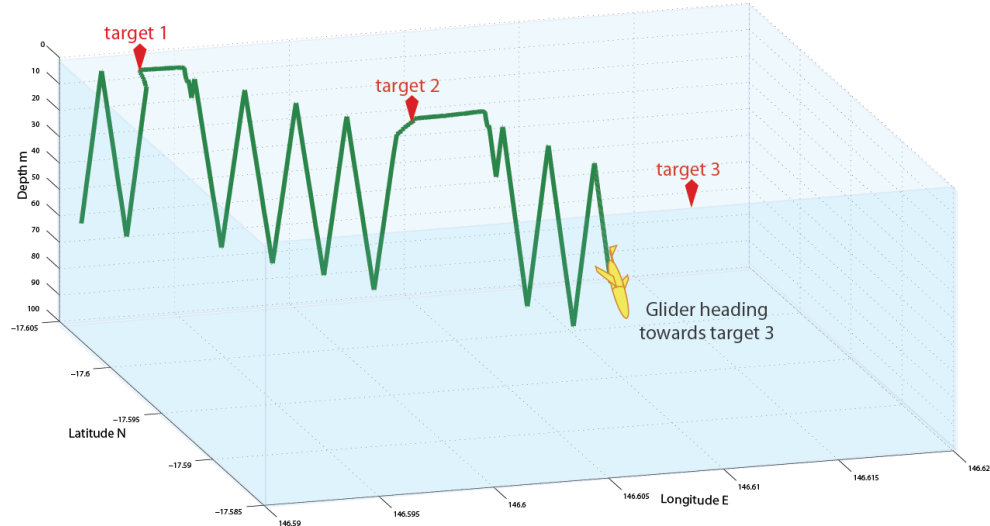


Figure 2 A Slocum glider performing 3 segments of saw-tooth lines. It surfaces at target points. This is different from a Seaglider, which usually surfaces after every descent-ascent cycle.

Seagliders, originally designed and built at the University of Washington, then manufactured by iRobot and now Kongsberg, are designed to operate most efficiently in the open ocean. ANFOG uses Seagliders to monitor the boundary currents surrounding Australia. The Seagliders are used to conduct repeated glider surveys across the boundary currents and continental shelves. As such, they are particularly valuable for gathering long-term environmental records of physical, chemical and biological data. Seagliders have an endurance of 1-6 months, range of 6,000 km and can sample up to 1000 m depth. Typically, the Seaglider surfaces after every dive-ascent cycle, takes GPS fixes and sends data. On some occasions, pilots may set the Seaglider to surface after a pre-determined number of dives have been completed in order to navigate through strong surface currents. Unlike

Slocum gliders for which only a subset of the dataset is transmitted while the glider is in the water (the full dataset will only be available for processing upon vehicle retrieval), Seagliders always send all their data at each surfacing. ANFOG Seagliders are equipped with a Seabird-CTD, WETLabs BBFL2VMT 3 parameters optical sensor (measuring Chlorophyll-a, CDOM and Backscatter) and a Seabird Oxygen sensor.

2.2 Known issues with sensors

2.2.1 Sea-Bird CTD recorder

All gliders used at ANFOG have been equipped with a Sea-Bird Conductivity Temperature Depth (CTD) recorder, optimized for low power consumption. Sea water salinity is computed using temperature, conductivity and pressure measurements acquired by this CTD. During the numerous ANFOG Slocum missions performed to date, two types of CTD sensors have been used: the CTD41CP before June 2011 and the GPCTD thereafter. Both these instruments sample at a rate of ~0.5Hz. Their principal difference is that the CTD41CP was an un-pumped CTD, whereas the GPCTD, which has been specifically designed for Slocum gliders and are now installed on all current ANFOG Slocum gliders, is equipped with a pump that allows for a constant flow inside the conductivity cell.

Sensor dynamics issues related to the typical profiling CTD, which were mainly high-frequency sampling CTD mounted on rosettes deployed from ships, have been described in the past (Horne and Toole (1980); Gregg and Hess (1985); Morison et al. (1994)). The issues usually manifest as spikes in salinity profiles as well as differences between a downward salinity profile and the following upward profile.

There are two main sources of data imperfections observed in salinity profiles: (i) different sensor time-responses of the thermistor, conductivity sensor and pressure sensor, and (ii) thermal lag effect. In the presence of differences in sensor time-responses, salinity is computed from pressure, conductivity and temperature measurement that don't match up with one another. The thermal lag effect is due to conductivity cell inertia: the conductivity used to compute salinity is measured inside a conductivity cell, which has the capacity of storing heat. Thus, the temperature used to compute salinity does not accurately reflect the temperature of the ocean, especially when the glider is flying through strong temperature gradients. The thermal lag issue was shown to be much reduced when the glider CTD was pumped, so that the flushed water sample is supposedly the same as the water sampled by the thermistor (Janzen and Creed 2011). However, in practice, the issue is still present in data from pumped CTDs (see examples below), although more easily correctable as the flow in the conductivity cell is known and constant.

2.2.2 Examples of Slocum CTD data problems seen in ANFOG data

In order to check validity of CTD data, it is appropriate to examine the quality of salinity data, since salinity is calculated from a combination of both temperature and conductivity (using TEOS-10 thermodynamic equation of seawater). Before correction, salinity spikes have been observed in Slocum CTD data near the thermocline (Figure 3 & Figure 4). This phenomenon is intensified in cases of strong gradients. In the example seen in Figure 4, Salinity spikes occur despite the absence of similar spikes in temperature and conductivity data (apart from ~18m depth, where a salinity spike is associated with a spike in conductivity).

Additionally, there is dissymmetry in the salinity profiles between up- and down-casts. As seen in Figure 5, negative spiking occurs in the downward profiles whilst positive spiking occurs in the upward profiles in the thermocline. During down-cast when temperature and salinity are decreasing with increasing pressure, negative salinity spiking is indicative of the conductivity signal leading the temperature signal (Sea-Bird Electronics, 2013).

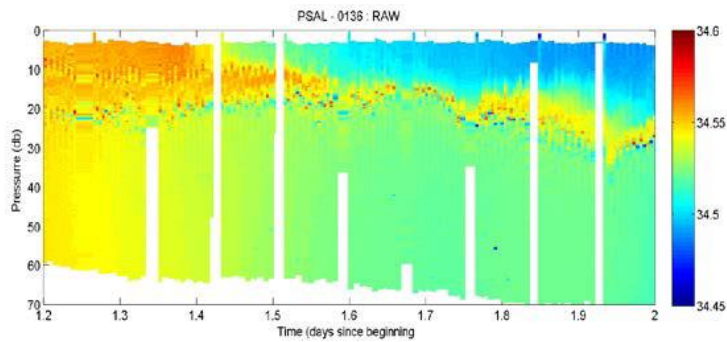


Figure 3 Salinity time-series data recorded during the first 2 days of a Kimberly deployment made by a Slocum glider in September 2012.

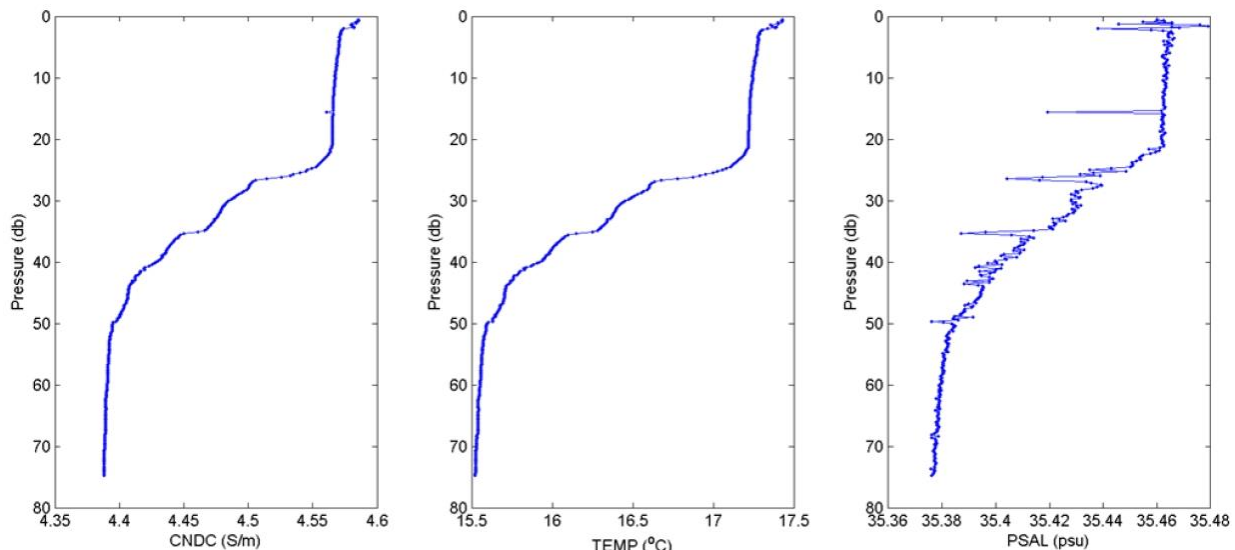


Figure 4 Associated Conductivity (left), Temperature (middle) and Salinity (right) downward profiles from a Yamba deployment (Sept 2012) (day 18.896).

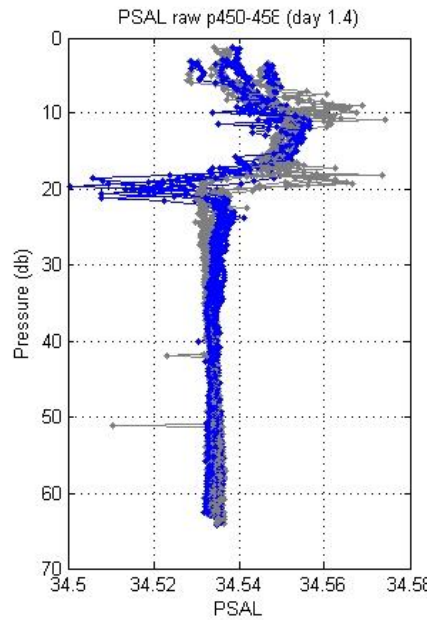


Figure 5 Four downward (blue) and four upward (grey) consecutive salinity profiles measured during the September 2012 Kimberly deployment.

Upon closer examination of Figure 5, it can also be seen that between 20db and 30db (20-30m depth), salinity measured on the descent is higher than that on the ascent. Such discrepancies are obvious on TS-diagrams, as can be seen in Figure 6 where data plotted from a series of four dives during the Yamba20120904 mission clearly exhibit a salinity difference of 0.05 psu when comparing glider descent with ascent. These differences result from thermal lag issues (Garau *et al.*, 2011).

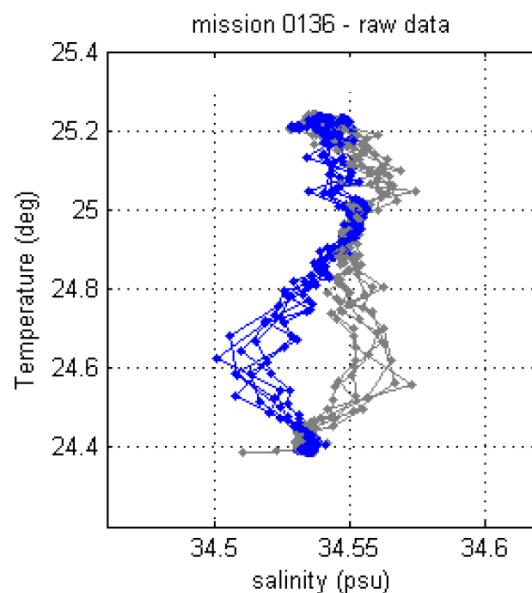


Figure 6 Temperature versus salinity plot for four down-casts (blue) and four up-casts of the September 2012 Yamba deployment.

2.2.3 Aanderaa Optode

ANFOG Slocum gliders are equipped with Aanderaa Optodes (3835 – 5013W). The following is the way in which the Optode internally computes dissolved oxygen concentration (in $\mu\text{mol/L}$).

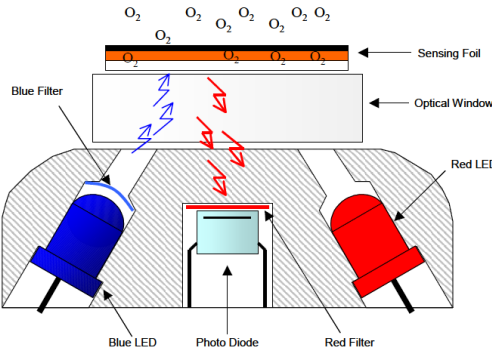


Figure 7 Optode optical design (Aanderaa, 2007).

The uncalibrated phase measurement (UNCAL_PHASE) is calculated as the difference between phase obtained with blue light excitation (BPHASE) and phase obtained with red light excitation (RPHASE) (Aanderaa, 2007; Thierry *et al.*, 2013):

$$\text{UNCAL_PHASE} = \text{BPHASE} - \text{RPHASE}$$

Since RPHASE is not used, it is set to zero.

Thus, $\text{UNCAL_PHASE} = \text{BPHASE}$

A calibrated phase (DPHASE) is calculated as a 3rd degree polynomial of UNCAL_PHASE (or BPHASE, in our case):

$$DPHASE = A + B \times BPHASE + C \times BPHASE^2 + D \times BPHASE^3$$

where A, B, C and D are the *PhaseCoef* calibration coefficients (C and D are usually equal to zero).

For Anderaa Optode 3930, 3835, 3975, 4130 and 4175:

DPHASE is then converted to dissolved oxygen concentration, MOLAR_DOXY ($\mu\text{mol/L}$), using additional foil-dependant coefficients in a 4th degree polynomial:

$$MOLAR_DOXY = C_0 + C_1 \times DPHASE + C_2 \times DPHASE^2 + C_3 \times DPHASE^3 + C_4 \times DPHASE^4$$

where C0, C1, C2, C3, C4 are temperature dependant coefficients calculated as:

$$C_i = C_{i0} + C_{i1} \times T + C_{i2} \times T^2 + C_{i3} \times T^3$$

T is temperature ($^{\circ}\text{C}$), and Cij are 20 foil-dependant calibration coefficients. One set of these 20 calibration coefficients is associated with each batch of foils.

For Anderaa Optode 4330, 4831, 4831 and 4835:

A few more steps are involved for the calculation of dissolved oxygen concentration, MOLAR_DOXY ($\mu\text{mol/L}$):

$$MOLAR_DOXY = \frac{C^* \times 44.659 \times AirSaturation}{100} \quad (1)$$

where C^* is oxygen solubility (cm^3/dm^3) is calculated from the Garcia & Gordon (1992) equation as:

$$C^* = \exp [A_0 + A_1 T_S + A_2 T_S^2 + A_3 T_S^3 + A_4 T_S^4 + A_5 T_S^5 + S (B_0 + B_1 T_S + B_2 T_S^2 + B_3 T_S^3) + C_0 S^2]$$

Where T_S is scaled temperature calculated by:

$$T_S = \ln \left(\frac{298.15 - t}{273.15 - t} \right)$$

t is temperature ($^\circ\text{C}$), and S is salinity, set to a constant 35 in our case¹.

$$\begin{array}{ll} A_0 = 2.00856 & B_0 = -6.24097e^{-3} \\ A_1 = 3.22400 & B_1 = -6.93498e^{-3} \\ A_2 = 3.99063 & B_2 = -6.90358e^{-3} \\ A_3 = 4.80299 & B_3 = -4.29155e^{-3} \\ A_4 = 9.78188e^{-1} & B_4 = -3.11680e^{-7} \\ A_5 = 1.71069 & \end{array}$$

Air saturation (%) in equation (1) is calculated by:

$$AirSaturation = \frac{\Delta p \times 100}{(NomAirPress - p_{vapour}) \times NomAirMix}$$

where NomAirPress is nominal air pressure = 1013.25 hPa,

NomAirMix is the nominal oxygen content in air = 0.20946,

¹ In future, we may consider applying CTD measured salinities instead of a constant 35. But at present, a constant value of 35 is preferred so as to avoid introducing spikes (seen in salinity data) into the dissolved oxygen data. Impact of varying salinity on the final oxygen data is small.

Δp is partial pressure of oxygen, calculated using DPHASE, temperature and polynomial calibration coefficients for the foil given by the manufacturer:

$$\Delta p = C_0 \cdot t^{m_0} \cdot DPHASE^{n_0} + C_1 \cdot t^{m_1} \cdot DPHASE^{n_1} + C_2 \cdot t^{m_2} \cdot DPHASE^{n_2} + \dots + C_{27} \cdot t^{m_{27}} \cdot DPHASE^{n_{27}} \quad (2)$$

where c, m and n are coefficients found in Aanderaa calibration sheets (see Table 1).

Table 1 Listing of relevant coefficients for equation (2) as found in Aanderaa calibration sheets.

Coefficients in equation (2)	Listing on Aanderaa sheet
$C_0 - C_{13}$	FoilCoefA
$C_{14} - C_{27}$	FoilCoefB
$m_0 - m_{27}$	FoilPolyDegT
$n_0 - n_{27}$	FoilPolyDegO

p_{vapour} is vapour pressure calculated from temperature t:

$$p_{vapour} = \exp \left(52.57 - \frac{6690.0}{t + 273.15} - 4.681 \times \ln(t + 273.15) \right)$$

Salinity compensation:

The dissolved oxygen concentration is also corrected for salinity effects. Salinity compensated MOLAR_DOXY is finally calculated as:

$$\text{MOLAR_DOXY}_{\text{SAL-compensated}} = \text{MOLAR_DOXY} * \exp [(S_{\text{set}}) (B_0 + B_1 T_S + B_2 T_S^2 + B_3 T_S^3) + C_0 * (S_{\text{set}})^2]$$

where Sset=35, in our case.

Early ANFOG Slocum deployments were performed with the glider configured such that only the internally computed dissolved oxygen data in $\mu\text{mol/L}$ were recorded. However, from May/June 2011, glider configuration settings were changed to “wphase” (sci_oxy3835_wphase_is_installed =1), allowing outputs of many more parameters. Thus, for deployments performed since mid-2011, the BPHASE, DPHASE and Optode temperature measurements have also become available. This is of critical importance for the improvement of oxygen data quality, as described in section 3.2.2.

2.2.4 Examples of Optode data problems seen in ANFOG Slocum data

A major issue in dissolved oxygen data is the disparity between up- and down-casts. For example, a sample of dissolved oxygen data recorded during the StormBay20120608 mission clearly shows a difference of up to 0.3ml/L (Figure 1). Moreover, after the Slocum glider has been parked on the surface, the dissolved oxygen values recorded upon the initial dive from the surface are often significantly higher. These two issues are due partly to problems with temperature values used in the computation of dissolved oxygen concentration from raw phase measurements. Indeed, looking at a plot of the Optode-measured temperature, there is evidently similar dissymmetry between up- and down-casts (Figure 9).

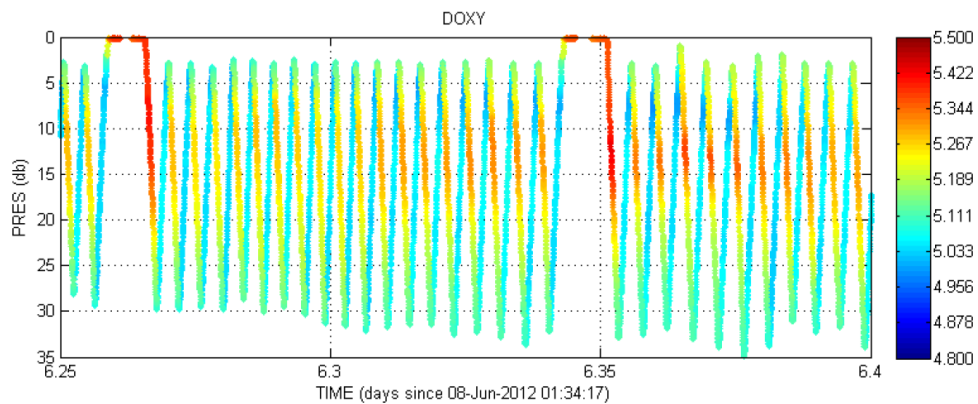


Figure 8 A sample of raw dissolved oxygen concentration (ml/L) time-series data taken from the June 2012 Storm Bay mission shows discrepancies between up- and down-casts.

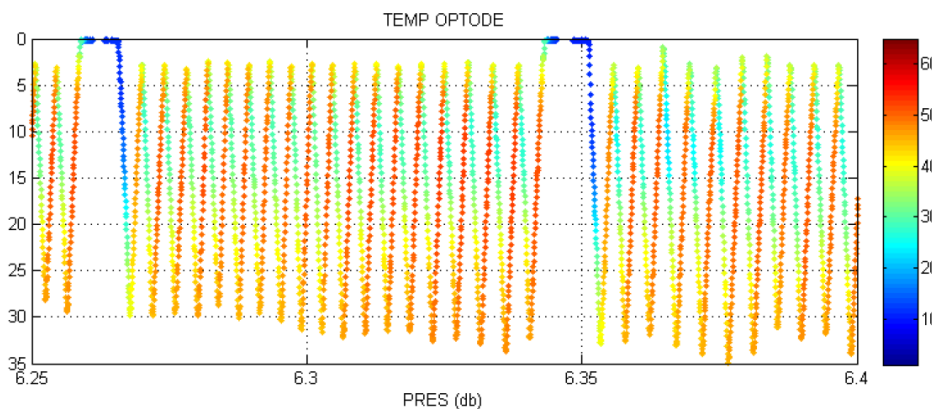


Figure 9 A sample temperature (°C) time-series data measured by the Optode during the June 2012 Storm Bay mission shows discrepancies between up- and down-casts.

Discrepancy between Optode-measured and CTD-measured temperature are especially pronounced whenever the glider traverses steep temperature gradients (Figure 10). Such an issue is well-known with Optodes because Optode temperature measurement is made inside the instrument rather than externally in ocean water. Recording of any major variations in ocean temperature is softened by instrument self-heating. Thus, the manufacturer recommends the use of temperature data from fast response temperature sensors when available to compensate for the temperature effect on oxygen (Aanderaa, 2007).

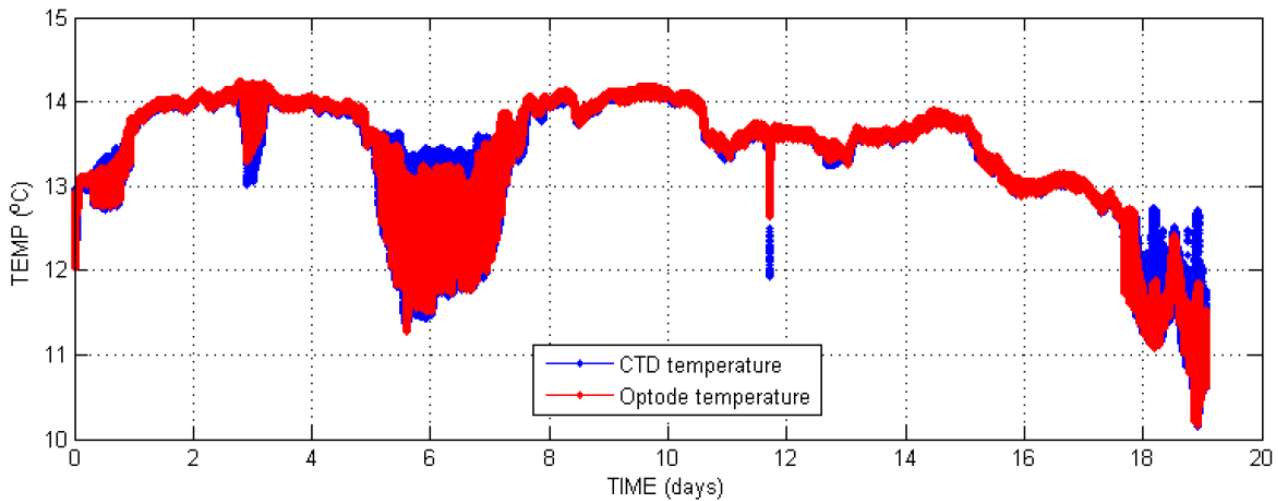


Figure 10 Temperature time-series data measured by the Optode (red) and CTD (blue) during the June 2012 Storm Bay deployment.

Another source of problem in dissolved oxygen data is the time response of the phase sensor, of the order of 20s, according to the manufacturer. Omitting to account for this time response induces a temporal mismatch between the different parameters used to compute oxygen. The effect of this time lag is obvious in Figure 11, where dissymmetry between up- and down-cast profiles highlights the lag in the BPHASE data.

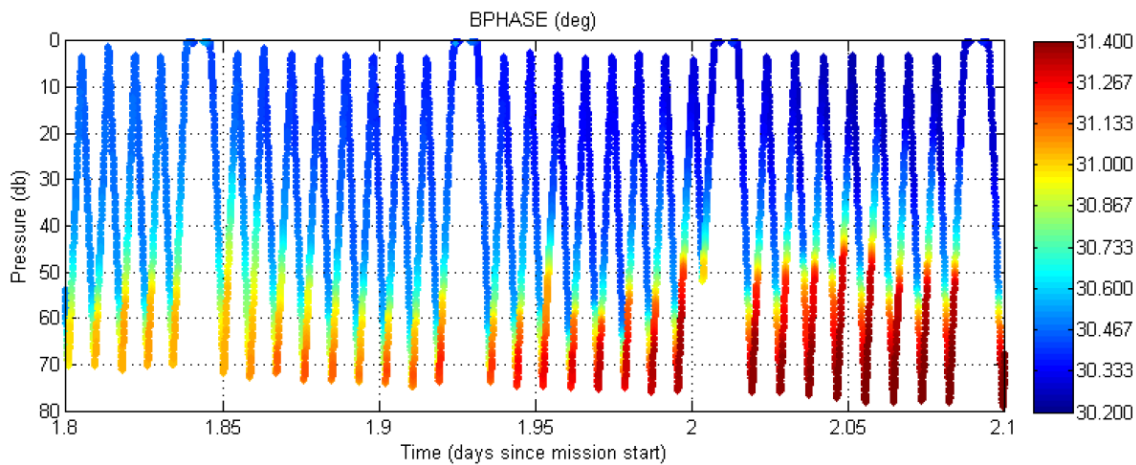


Figure 11 Raw BPHASE measurements taken from the Kimberley Mission conducted in July 2012 show dissymmetry between up- and down-casts.

ANFOG Seagliders are equipped with Seabird SBE_43FO2 oxygen sensors and Seabird CT (SBE_CT) sensors. Although these CTD are not pumped, dissymmetry such as that seen with Slocum glider data is not typically observed because Seagliders travel more slowly through the water, and the dive and climb profiles are very widely spaced, with surfacings 6 km apart during dives to 1km depth (Frajka-Williams, 2011).

2.2.5 Bio-optical Sensors

All gliders at ANFOG are equipped with WETLabs ECO Puck triplets which incorporate scattering meters to measure Chlorophyll-a fluorescence, coloured dissolved organic matter (CDOM) fluorescence and backscattering. The scattering meter sensors have a 117° centroid angle and a single LED light source and detector. Specifically, the older Slocum gliders were fitted with WETLabs BBFL2SL and BBFL2VMT, which function at wavelengths of 650nm or 660nm. These sensors were replaced with FLBBCDSLK and FLBBCDSL, which function at a wavelength of 700nm. Seagliders are fitted with WETLabs BBFL2VMT also. Additionally, the Slocum gliders are also fitted with Satlantic OCR-504 Multispectral Radiometers to measure downwelling spectral irradiance at 4 frequencies.

The parameters for Chlorophyll-a concentration (CPHL), CDOM concentration (CDOM), Volumetric Backscatter Coefficient (VBSC) and downwelling spectral irradiance (IRRADxxx²) are computed using raw measurements made in counts and the associated calibration coefficients and dark count values, i.e.:

$$\text{PARAM}_{\text{units}} = \text{SF} \times (\text{PARAM}_{\text{counts}} - \text{DC})$$

where SF is scale factor coefficient, DC is dark count coefficient.

For downward spectral irradiance, there is an additional scaling factor (IRRAD_IC) according to the chosen wavelength:

$$\text{PARAM}_{\text{units}} = \text{IRRAD_IC} \times \text{SF} \times (\text{PARAM}_{\text{counts}} - \text{DC})$$

Scale factors and dark count coefficients are obtained from independent laboratory-based calibrations performed by each instrument's respective manufacturer.

Additionally, VBSC is converted to Particle Backscatter Coefficients (BBP) during delayed mode processing. Details of how this is done are available in Mantovanelli & Thomson (2016). Basically, Matlab code developed by Zhang *et al.* (2009)³ is used to calculate seawater volumetric scattering, β_{sw} . Input comprises the wavelength of the sensor (650 – 700nm, depending on the model used), censor centroid angle (117° recommended by Boss & Pegau (2001)), depolarization ratio (0.039 used by default by Zhang *et al.* (2009) based on Farinato and Roswell (1976)), and CTD temperature and salinity.

² The parameter is named according to the wavelength of the beam, i.e. IRRAD443 for the wavelength closest to 443nm. The actual wavelength which may vary slightly from 443nm is specified in the 'comment' attribute of the parameter.

³ Zhang et al. (2009) Matlab code is available to the public at http://www1.und.edu/faculty/zhang-xiaodong/_files/docs/programs/betasw_zhh2009.m

Particle backscatter coefficient, BBP, is then computed as follows:

$$BBP = 2\pi \times (VBSC - \beta_{sw}) \times X_p$$

where $X_p = 1.1$ (recommended by WETLabs 2013)

2.2.6 Examples of bio-optical data problems seen in ANFOG Slocum data

Dark counts in bio-optical instruments can be affected by various environmental (e.g. temperature) and platform dependent (e.g. power) parameters (Cetinic *et al.*, 2009). As such, applying the lab-determined value sometimes leads to an inordinately large proportion of negative values calculated. For example, application of the lab calibrated darkcount resulted in an unacceptable 93.6% of the calculated CDOM values being negative (depicted as the blank areas in Figure 12).

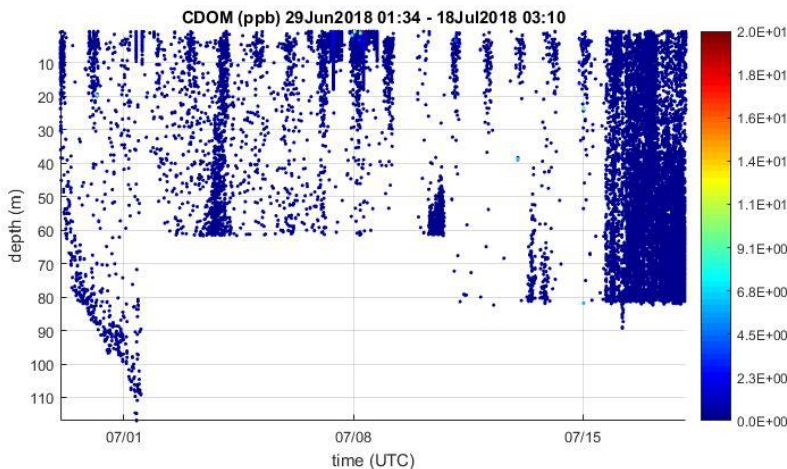


Figure 12 Uncorrected CDOM time-series data from Forster20180629 mission with 93.6% of values being negative (seen as the white spaces).

Another problem with optical sensors deployed in the oceans around Australia is their susceptibility to biofilm and barnacle growth (Figure 13), depending on the duration, location of deployment and type of fouling. Just 10% coverage of the optical path will affect the quality of data strongly, resulting in noisy data which may be enhanced or damped (Lehaitre *et al.*, 2008, Cetinic *et al.*, 2009).



Figure 13 Examples of biofouling growing on the windows of optical sensors in a (left) Slocum glider and (right) Seaglider.

In the example shown in Figure 14, noise generated from the gradual growth of biofouling starts to completely take over the Chlorophyll-a fluorescence signal 3 weeks into the TwoRocks20170512 mission off Perth.

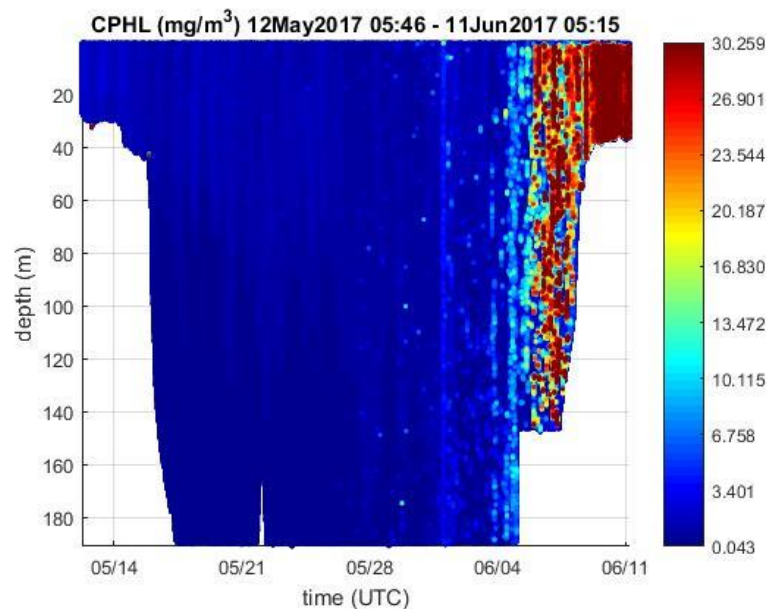


Figure 14 Biofouled optical sensor at the end of the mission (TwoRocks20170512) is seen as severely raised values in the chlorophyll-a fluorescence time-series data.

3 Delayed-mode QA/QC

This section describes the main delayed mode QA/QC procedures for the data that has been extracted from .dbd and .edb files of Slocum gliders, and .log and .eng files of Seagliders, which falls within the step circled red in Figure 15. Subsequently, the completed NetCDF files are uploaded to AODN to be checked, stored and made available to the public online, along with the associated QA/QC report and data plots.

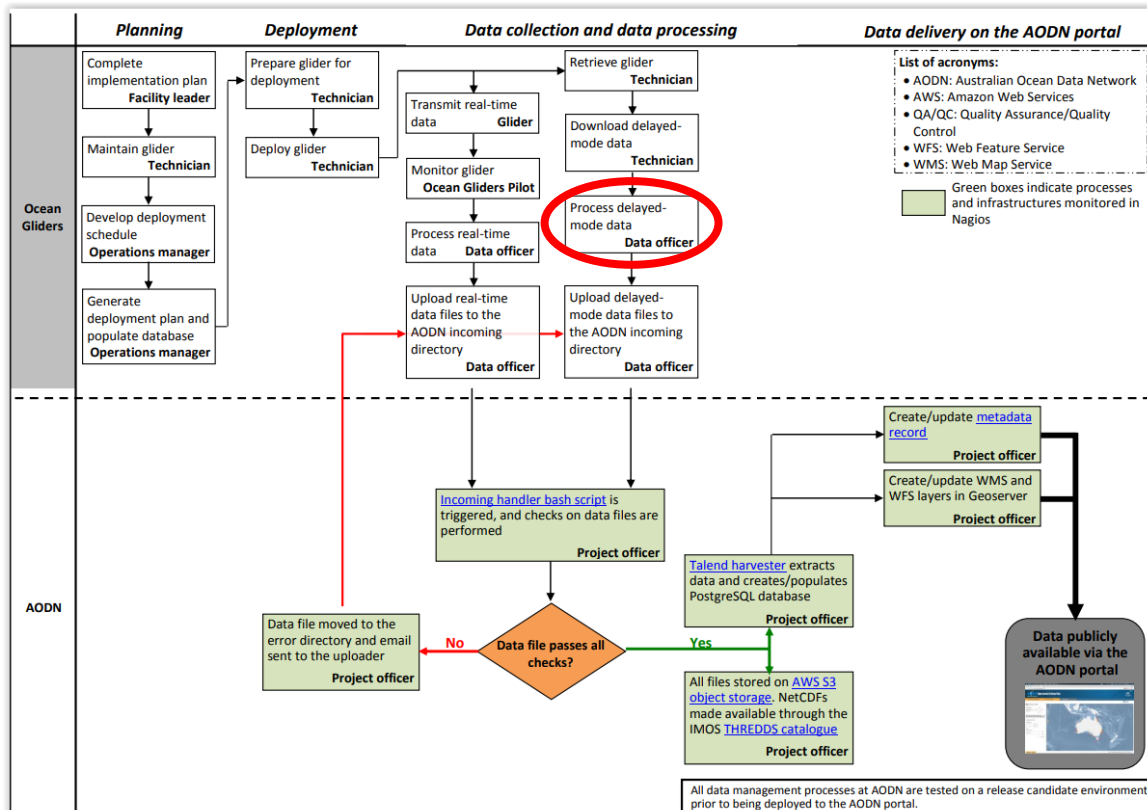


Figure 15 Workflow of ANFOG glider data. Red circle highlights the part covered in this document. (AODN Portal User Guide Public Documents, 2016).

3.1 Glider data and metadata format

Firstly, the proper data file structure must be set up and populated with the sufficient metadata to make the data in each NetCDF file self-described. ANFOG delayed-mode format files contain metadata and scientific data for one deployment of one glider. Since the advent of delayed mode processing version 4.0, ANFOG has generated NetCDF-4 format files (versus NetCDF-3 format previously), and released 2 types of NetCDF files for each deployment: FV00 and FV01. These two files contain the same global attributes. The FV00 file contains all the raw data from the deployment (both in engineering and physical units), with each parameter following its own time dimension. Data in FV00 files are not quality controlled. The FV01 file is the one recommended to users, with all

parameters associated with quality control flags. The FV01 file contents include corrected data and also parameters which have been interpolated (slightly, as all the time dimensions are usually very similar) following the same unique time dimension.

ANFOG delayed-mode NetCDF files comply with Climate and Forecast (CF) Metadata Conventions v1.6 and IMOS conventions v1.4. Users are directed to the Australian National Facility for Ocean Gliders (ANFOG) Data Management Users' Manual (Woo *et al.*, 2018) for detailed information on the ANFOG glider data and meta-data format.

Download:

ANFOG Data Management Manual

<http://imos.org.au/facilities/oceangliders/glider-data/>

3.2 Automated data corrections

In version 4.0 and above of ANFOG data processing, the ANFOG Data Officer can choose to apply corrections on Slocum CTD and Optode data. Indeed, the Seaglider processing chain has always included scripts developed by the University of Washington where thermal lag and small scale time lags are taken into account in salinity computation. However, in Slocum data processing, before version 4.0, these considerations were missing. This section discusses automated corrections made to Slocum CTD and Optode data. Additionally, basic corrections to biogeochemical data are also shown.

3.2.1 CTD corrections

Work presented by Bishop (2008), Garau *et al.* (2011) and Kerfoot *et al.* (2006) are used for automatic CTD corrections. In order to correct erroneous spiking seen in salinity values discussed in section 2.2.2, a 3-step automated correction process is employed (Figure 16).

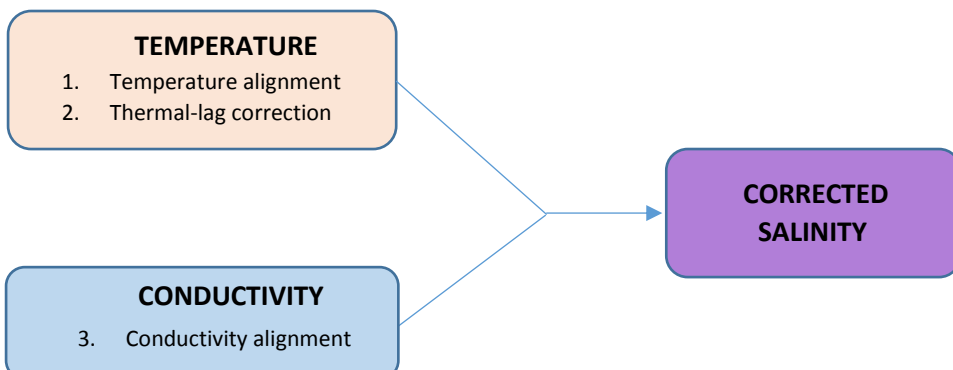


Figure 16 Schematic of 3-step process to correct CTD data.

The first step (section 3.2.1.1) takes into account the temperature sensor time response and re-aligns the temperature with pressure (assuming that the pressure sensor time response is negligible). Once the best correction for temperature has been defined, we use this corrected temperature in step 2 (section 3.2.1.2) to estimate the temperature inside the conductivity cell as part of the thermal lag correction, and then finally in step 3 (section 3.2.1.3) correct the conductivity misalignment, looking for the best salinity match.

3.2.1.1 Temperature alignment

Temperature is first corrected (independent of salinity) by finding the best match between down- and up-cast profiles of temperature. A linear time shift is applied to the temperature data based on a method described in Kerfoot *et al.* (2006) where they computed mean temperature profiles of 100 up-casts and 100 down-casts and compared the two mean profiles, time-shifted from 0 to 5 seconds by intervals of 0.1 seconds. The time shift value which gave the best match between the mean downcast and mean upcast profiles could then be determined. At ANFOG, a similar method is applied, except that data from the entire mission is used.

The procedure is as follows:

- 1) At each 0.1 s time shift, RMS difference and BIAS values are computed for every pair of descent and ascent profile, and the median found;
- 2) The process is repeated for each subsequent time shift, resulting in a graph like Figure 17.
- 3) The temperature data is then corrected using the time shift that results in the smallest absolute BIAS (seen as the minimum point on the blue curve).

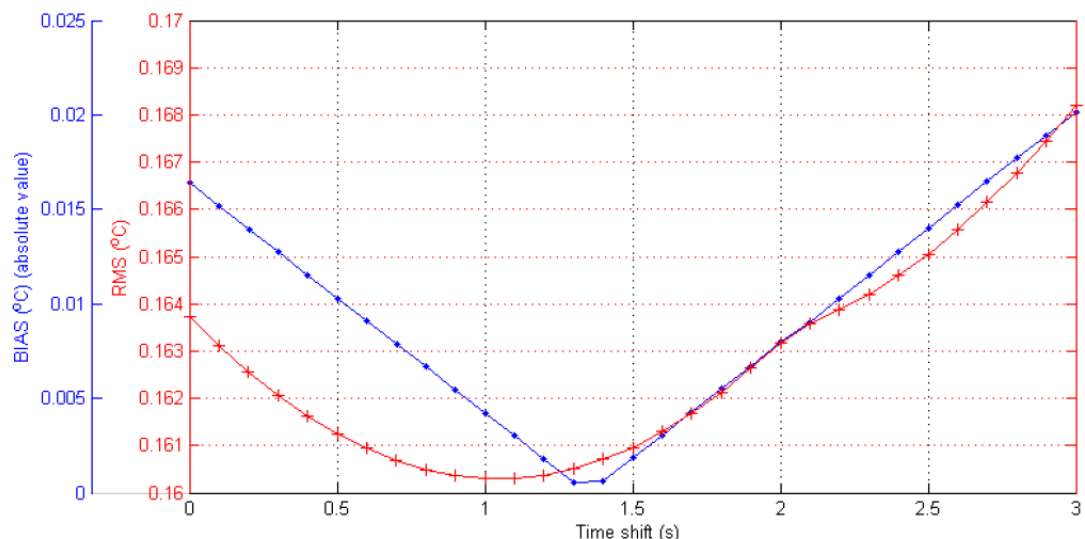


Figure 17 Absolute value of the median BIAS and the median RMS difference between up- and down-cast temperature profiles for the Yamba October 2013 mission, as a function of time shift.

There is usually only little difference between the minimum RMS difference and BIAS (0.2s in this case). Because the reduction in RMS difference between the original value and the minimum value is proportionally very small, the minimum BIAS value is chosen over the RMS difference value. However, both are calculated for verification purpose.

3.2.1.2 Thermal lag correction

3.2.1.2.1 Pumped CTD

In the case of pumped CTD recorders, flow through the conductivity cell is known and constant, so we can easily apply the method of Lueck and Picklo (1990), generalised by Morison et al. (1994), which estimates temperature inside the conductivity cell and uses this temperature to compute salinity, rather than the thermistor temperature measured outside the cell. According to Lueck and Picklo (1990) the temperature inside the cell can be estimated by applying the following recursive filter:

$$(n) = -bT(n-1) + a [(n) - T(n-1)] \quad (1)$$

Where T_T is the temperature correction subtracted from the measured temperature T , n is the sample index, and the constants a and b are:

$$a = 4f_n\alpha\tau / (1 + 4f_n\tau) \quad \text{and} \quad b = 1 - 2a/\alpha$$

Where f_n is the Nyquist frequency, i.e. half the CTD sampling interval (Kerfoot et al., 2006).

Morison et al. (1994) show that if the flow in the conductivity cell is constant, α and τ can be estimated using the following empirical relation:

$$\alpha = 0.0264 V^{-1} + 0.0135 \quad \text{and} \quad \tau = 2.7858 V^{-1/2} + 7.1499 \quad (2)$$

In the case of GPCTD recorders used in ANFOG Slocum gliders, the flow rate in the conductivity cell is 10 ml/s, the volume of the cell is 3 ml and its length 146mm, which gives a velocity:

$$V = 0.4867 m s^{-1}$$

As this velocity falls within the valid range stated by Morison et al. (1994), a and b can then be computed and the temperature inside the conductivity cell derived using equations (2) and (1).

3.2.1.2.2 Unpumped CTD

When correcting data from unpumped CTD, α and τ from equation (2) are computed by estimating that velocity for each profile is the same as the glider velocity of travel through the water column. Temperature within the conductivity cell is then calculated by applying equations (1) and (2).

This method was chosen over the method proposed by Garau *et al.* (2011) which had been formulated as an improvement of the commonly used Morison *et al.* (1994) method so as to take into account for variable flow speed inside the conductivity, irregular sampling intervals etc., as an un-pumped glider-mounted CTD would have. However, our testing found that using their method did not lead to better results than when recomputing α and τ using an estimate of the glider's velocity across the water column, V , per profile. Moreover, their method was time consuming, especially when taking into account the conductivity sensor time response, which forced us to perform many iterations to get the best parameters and time lag.

3.2.1.3 Conductivity alignment

Conductivity time lag is estimated after the completion of salinity alignment and thermal lag correction. It was found that conductivity time lag is not constant throughout the whole deployment. It is speculated that this may be due to geometrically induced time lag, i.e. the conductivity cell is a distance away from the pressure sensor, and pitch and dive rate of the glider are too variable on a single profile. Our efforts to correct for geometric time lag failed. The method employed for conductivity alignment which brought good results is as follows:

- 1) Determine the time shift in conductivity data that produces the best match (smallest RMS difference) for each individual pair of computed salinity up- and down-cast profile (values tested at increasing 0.1s time shift intervals). The RMS difference is used for this estimate rather than the BIAS value, due to the presence of spikes in salinity profiles which can change the sign of the BIAS difference between the 2 profiles of a dive-climb pair.

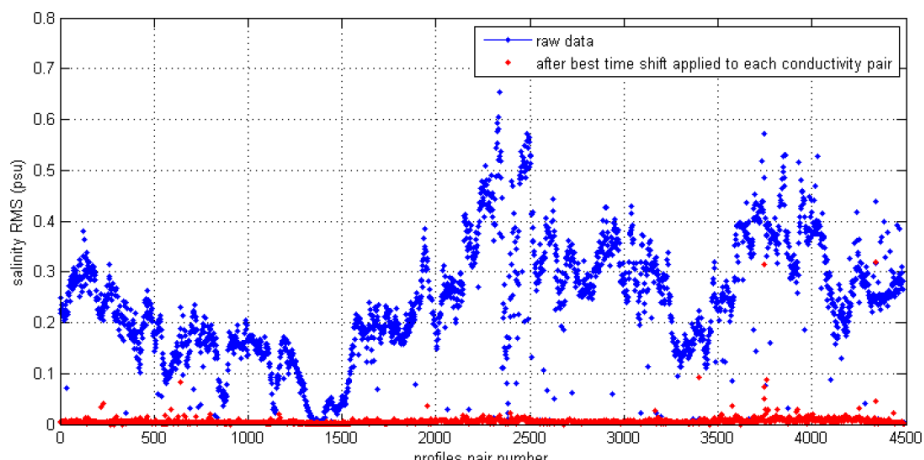


Figure 18 Salinity RMS difference between consecutive up- and down-cast pair is greatly reduced by the introduction of a best time shift in conductivity data for each individual pair.

In the Yamba20120904 mission for instance, applying the best time shift for each individual dive-climb pair in conductivity data, successfully decreases the salinity RMS difference significantly from values of the order of 0.1 psu (blue dots) to the order of 0.01 psu (red dots) (Figure 18).

- 2) When a best time shift for conductivity has been determined for each and every individual dive-climb pair, their median is found (Figure 19) and applied to the entire conductivity time-series dataset to correct its alignment.

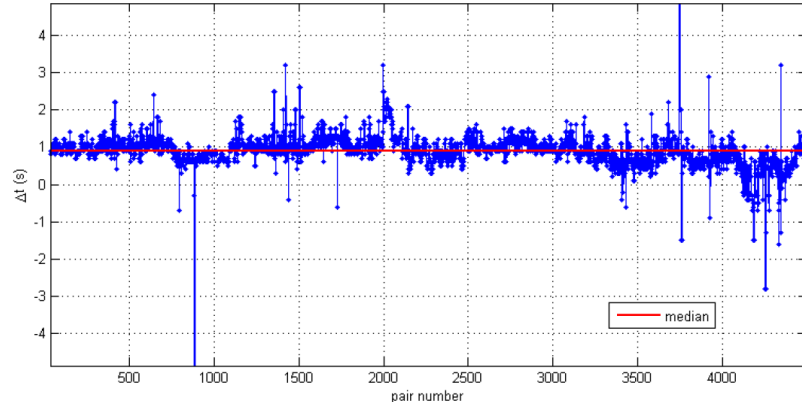


Figure 19 Conductivity time delay (in seconds) by pair of profiles, from beginning of the Yamba20120904 mission (left) to the end mission (right). The red line is the median time shift (0.9s here).

The effect of the abovementioned CTD corrections can be seen in Figure 20 where time lag corrections and thermal lag correction are applied separately to data from the Kimberley20120914 mission CTD data.

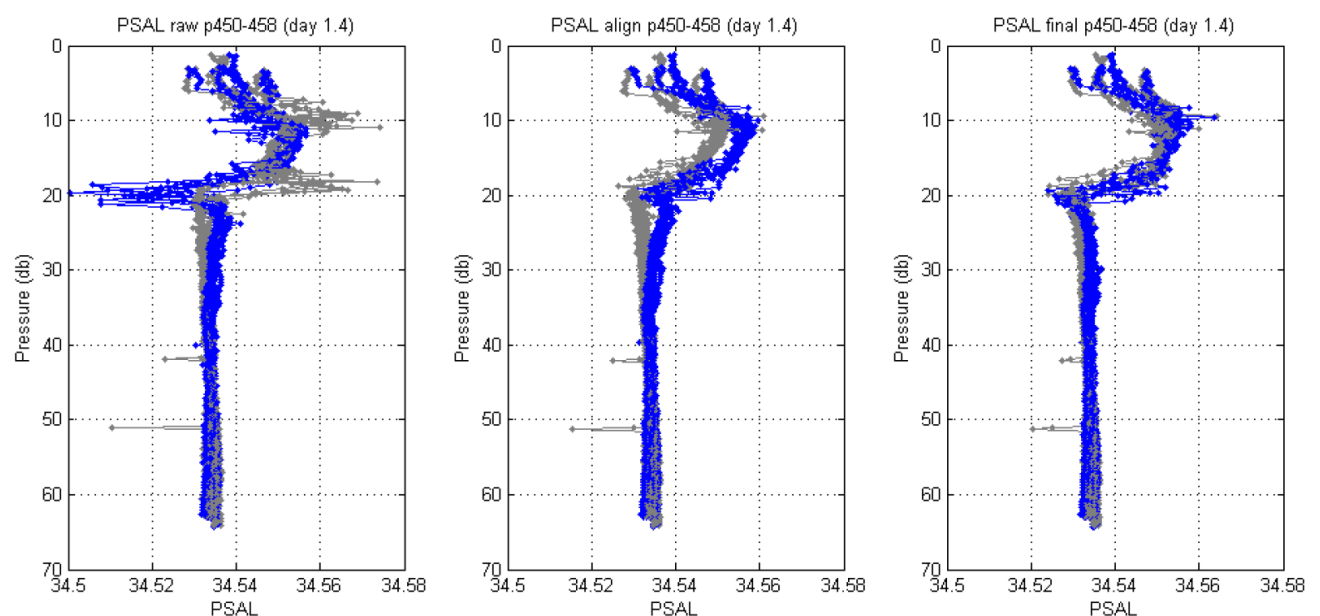


Figure 20 (Left) Uncorrected raw salinity data from 4 profile pairs, (middle) only temperature and conductivity alignments corrected, (right) thermal lag corrected as well as temperature and conductivity alignment.

Comparing the three plots in Figure 20, it can be seen that the erroneous spikes seen in raw data (left plot) are significantly reduced by corrections in temperature and conductivity alignment (middle plot). And this is improved further with the addition of thermal lag correction (right plot).

As a result of these corrections, much of the salinity spiking problems described in section 2.2.2 can be largely minimised (see Figure 21).

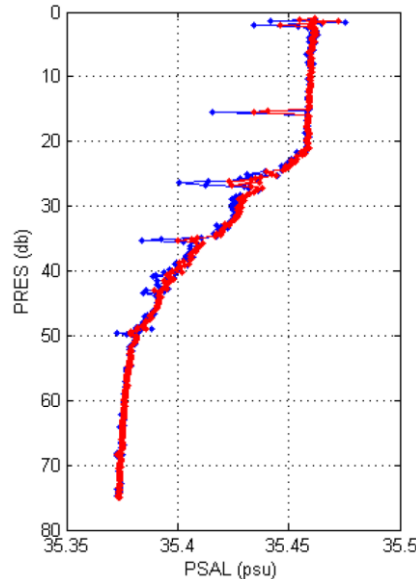


Figure 21 Salinity profile no. 4114 from the Yamba20120904 mission: (blue) raw salinity, (red) corrected salinity.

3.2.2 Oxygen Optode corrections

To improve dissolved oxygen data (MOLAR_DOXY, as internally computed by the glider), re-computed must be performed using corrected Optode BPHASE measurements, corrected CTD temperature data and Optode calibration coefficients provided by Aanderaa for each sensor⁴.

The CTD temperature has now been corrected for short term mismatch with the CTD pressure (see section 3.2.1.1), so BPHASE data must also be aligned with pressure. Moreover, because the Optode is separated from the pressure sensor by a distance of 90cm on the Slocum glider (Figure 22), at typically slow speed of glider travel, this distance induces a non-negligible time difference between when the pressure and the BPHASE measurements are recorded, which needs to be accounted for (3.2.2.1). Subsequently, the lag resulting from BPHASE sensor response time must also be minimised (3.2.2.2). Finally, we combine this corrected BPHASE data with the CTD temperature and the calibration coefficients, to get the final corrected dissolved oxygen data, in $\mu\text{mol/L}$.

⁴ For this re-computation to be possible, both the temperature and BPHASE data must share the same time axis, thus linearly time-interpolated CTD temperature is used.

3.2.2.1 Geometrical alignment

On Slocum gliders, the Optode is installed aft, close to the fin, and the CTD is installed toward the middle of the glider, close to the wings (Figure 22).

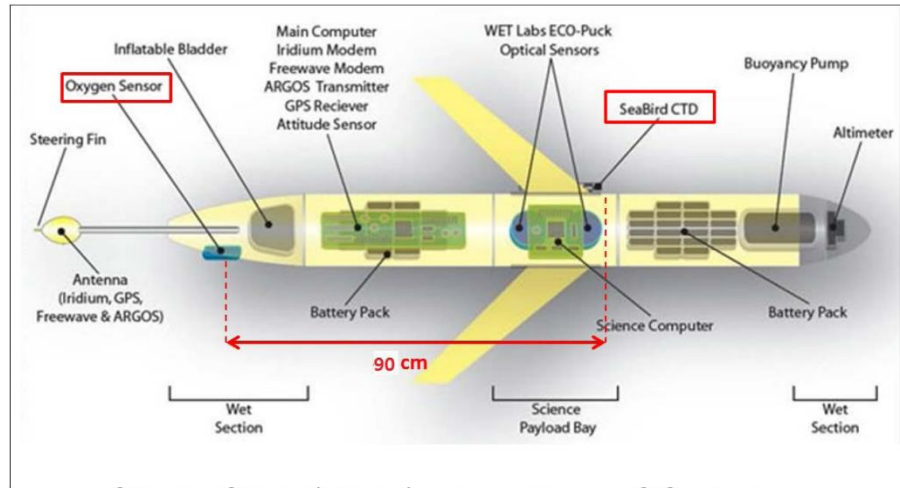


Figure 22 Schematic diagram of Slocum glider (After AUVAC, 2018).

The time, τ , taken to travel the 90cm distance between the Optode and CTD recorder is:

$$\tau = \frac{d}{v}$$

where d is the distance between the sensors and v is the glider velocity of travel, i.e.

$$v = \frac{r}{\sin \theta}$$

where r is dive rate (m/s) and θ is glider pitch.

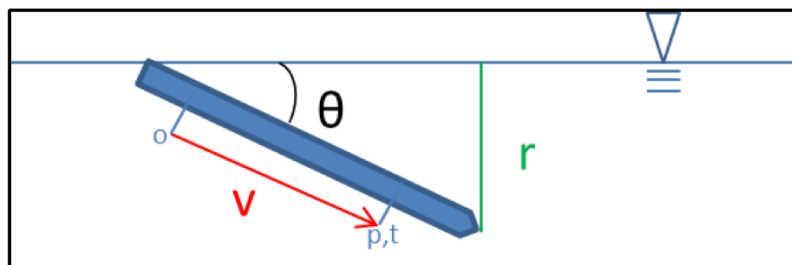


Figure 23 Glider orientation during descent. (p: pressure, t: temperature, o: oxygen)

Thus, the time delay between oxygen (or BPHASE) and pressure is:

$$\tau = \frac{d \cdot \sin\theta}{r}$$

Applying the measured distance between the sensors $d = 0.9\text{m}$, and ideal values for glider travel, $r = 0.1 \text{ m/s}$, $\theta=26^\circ$,

$$\tau = 3.9450 \text{ s}$$

However, in practice, the glider travels with varying pitch and dive rate. Depending on the ballast, the average pitch (in absolute value) on dives can significantly depart from the average pitch on climbs, so the time delay, τ , also varies between dive and climb. Therefore, in order to account for this, τ is found for each cast using the average pitch and dive rate on that particular cast. Then, the results for the whole mission are filtered to avoid extreme values (e.g. see Figure 24). Finally, using the filtered values of τ , a linear time shift is applied to the BPHASE data to correct for geometrical alignment.

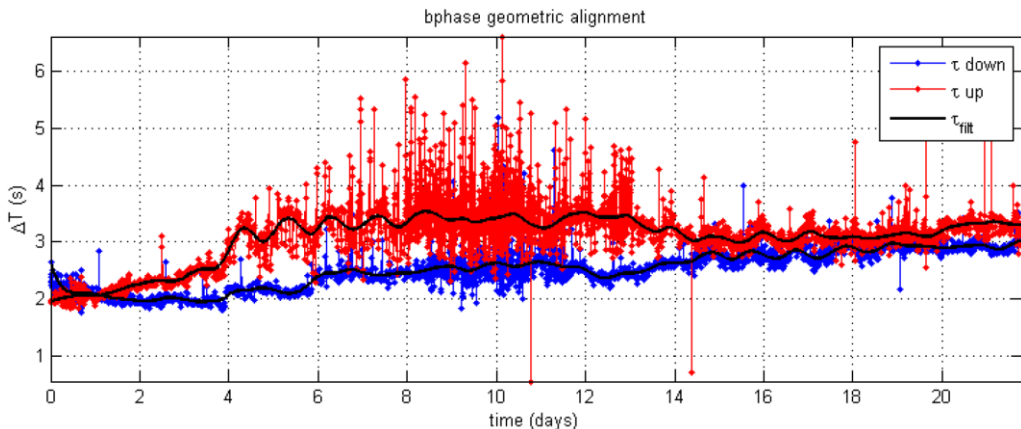


Figure 24 Time lag between BPHASE and pressure measurements, as a timeseries over the course of the Kimberley20120727 mission. Blue: down-cast, Red: up-cast, Black: filtered values.

3.2.2.2 Time lag correction

Time taken for the Optode sensor to respond while taking measurements results in a time lag that must be corrected. The lag is relatively long (of the order of 20s, according to the manufacturer). A similar method to that previously used for correcting CTD temperature time lag is also applied here to correct the time lag in the Optode BPHASE:

- 1) At each 1 s time shift, RMS difference and BIAS values are computed for every pair of descent and ascent profile, and the median found;
- 2) The process is repeated for each subsequent time shift, resulting in a graph like Figure 25.
- 3) The BPHASE data is then corrected using the time shift found to result in the smallest RMS difference value (e.g. 26s for the Kimberley20120727 mission (Figure 25)).

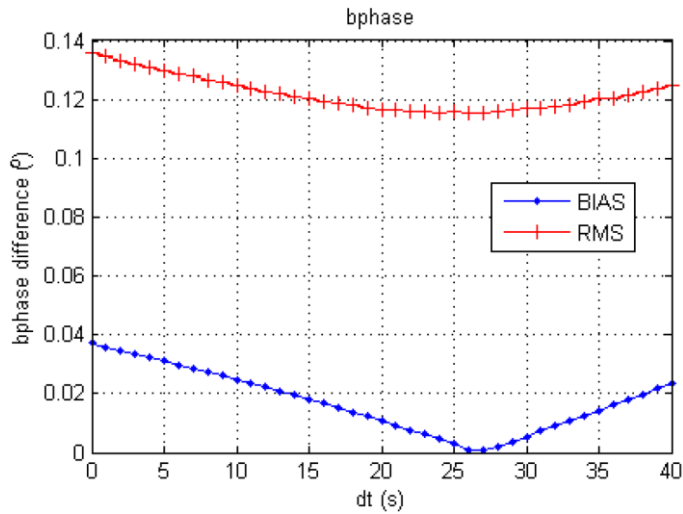


Figure 25 Median values of RMS (red) difference and BIAS (blue) between up- and down-cast BPHASE (in degrees) data, plotted against time shifts applied, for the Kimberley20120727 mission.

For data from the Kimberley20120727 mission, a linear time shift of 26s minimised the dissymmetry previously seen in the raw BPHASE data (Figure 26).

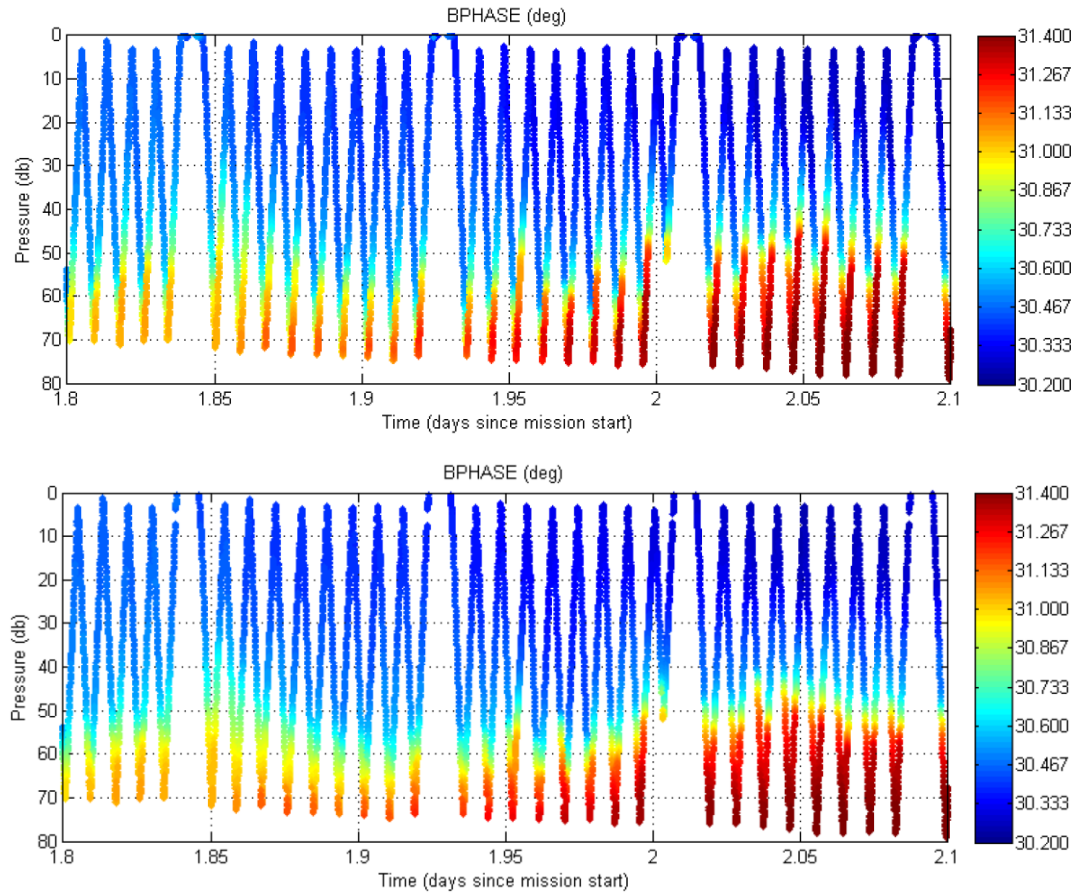


Figure 26 (Top) Uncorrected BPHASE data exhibiting dissymmetry between up- and down-casts; (bottom) symmetry between up- and down-casts is improved by 26s time lag correction.

With BPHASE corrected for geometrical lag and sensor time lag, the concentration of dissolved oxygen is finally re-computed as described in section 2.2.3, using manufacturer calibration coefficients, temperature data from the CTD instead of from the Optode (time interpolated to match with the Optode BPHASE), and with compensation for salinity effects also applied.

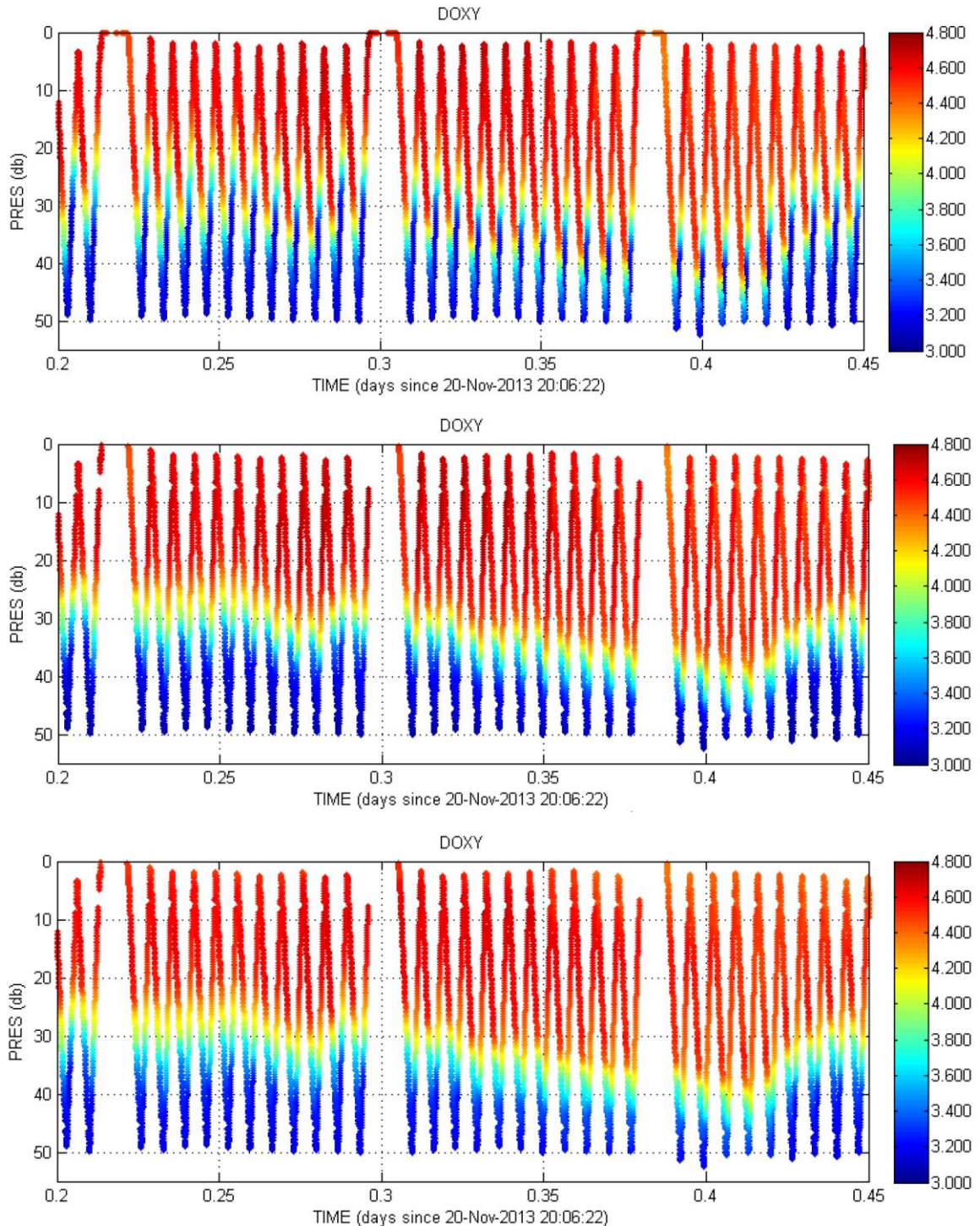


Figure 27 Dissolved oxygen concentration time-series profiles that are (top) uncorrected, (middle) recomputed with geometrical and sensor lag corrections, and (bottom) recomputed using CTD temperature and corrected for geometrical and sensor lags.

From Figure 27, it can be seen that the uncorrected dissolved oxygen data directly reported by the Optode (top plot) is significantly improved by corrections to BPHASE to account for geometrical and sensor lags (middle plot). Data on dive and climb profiles become much more symmetrical. Substituting Optode temperature data with CTD temperature in calculations further improves the quality of the oxygen data (bottom plot).

In future, our Optode data corrections will include the application of pressure compensation also (as recommended by the manufacturer).

This will involve multiplying the oxygen concentration by a factor F:

$$F = 1 + \frac{0.032 \times \text{pressure}}{1000}$$

where pressure is measured in dbar.

The pressure effect is small in shallow water ($F=1.0064$ for 200db), but becomes more significant for deep Slocum missions where the glider reaches pressures of up to 1000db.

3.2.3 Bio-optical data corrections

No automatic corrections to bio-optical data are applied if less than 1% are negative values. Otherwise, the factory calibrated dark count value is corrected. This is performed to Chlorophyll-a, CDOM fluorescence and downwelling spectral irradiance data by iteratively decreasing the dark counts until less than 1% of computed values are negative. Subsequently, the corrected data are recomputed using the new dark count according to the method described in section 2.2.5.

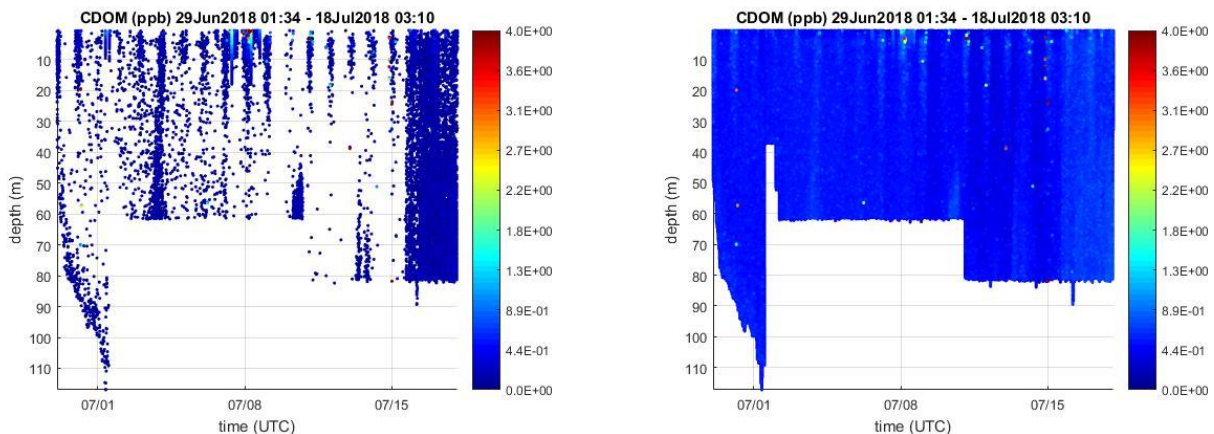


Figure 28 CDOM timeseries data (left) calculated with factory calibrated dark count, and (right) with corrected dark count.

Using the factory calibrated CDOM dark count of 47 to compute CDOM values for the Forster20180629 mission resulted in loss of 93.55% of CDOM data (Figure 28, left). It was found that 41 was a more suitable dark count value, resulting in 0.21% of recomputed CDOM data being negative (Figure 28, right).

4 Automatic Quality Tests

This section describes a series of QC tests that are automatically run to flag scientific data. The QC flagging convention applied is described in detail by the ANFOG Data Management document (Woo *et al.*, 2018).

4.1 Impossible date test

The impossible date test checks that time values are within the timeframe associated with the deployment (defined in the *deployment_start_date* and *deployment_end_date* attributes of the variable *DEPLOYMENT*). All data outside of this timeframe are removed.

4.2 Impossible location test

The impossible location test requires that the latitude and longitude that position the observations are sensible. LATITUDE or LONGITUDE data that fail this test are flagged with 4 (Table 2).

Latitude in range -90 to 90 degrees

Longitude in range -180 to 180 degrees

Good scientific data measured at locations that are bad or missing receive a flag of QC=3.

Table 2 IODE⁵ flags used in flagging ANFOG glider data

Flag value	Meaning	Description
0	No QC performed	The level at which all data enter the working archive. They have not yet been quality controlled.
1	Good data	Top quality data in which no malfunctions have been identified and all real features have been verified during the quality control process.
2	Probably good data	Good data in which some features (probably real) are present but these are unconfirmed. Code 2 data are also data in which minor malfunctions may be present but

⁵ IODE is the International Oceanographic Data and Information Exchange.

		these errors are small and/or can be successfully corrected without seriously affecting the overall quality of the data.
3	Bad data that are potentially correctable	Suspect data in which unusual, and probably erroneous features are observed.
4	Bad data	Obviously erroneous values are observed.
5	Value changed	Altered by a QC centre, with original values (before the change) preserved in the history record of the profile.
6	Not used	Reserved for future use.
7	Not used	Reserved for future use.
8	Interpolated value	Indicates that data values are interpolated.
9	Missing Value	Indicates that the element is missing.

4.3 Range test

The range test applies a gross filter on observed values for the measured scientific parameters which must accommodate all expected extremes encountered in the oceans around Australia. Valid maxima and minima as listed in Table 3 are tested, except for the engineering parameters HEAD, UCUR and VCUR for which no QC is performed (QC flag = 0). A QC flag of 4 is applied to data that fail this test.

Table 3 Gross limits applied to parameters measured by sensors on ANFOG gliders.

code	standard_name / long_name (for non-CF)	valid_min	valid_max	units
CNDC	sea_water_electrical_conductivity	0	60	S m ⁻¹
TEMP	sea_water_temperature	-2.5	40	Celsius
PRES	sea_water_pressure	-5	1100	dbar
BBP	particle_backscattering_coefficient	0	1	m ⁻¹
PSAL	sea_water_salinity	2	41	1e ⁻³

DOX1	mole_concentration_of_dissolved_molecular_oxygen_in_sea_water	0	650	umol l ⁻¹
DOX2	moles_of_oxygen_per_unit_mass_in_sea_water	0	650	umol kg ⁻¹
CPHL	mass_concentration_of_chlorophyll_in_sea_water	0	100	mg m ⁻³
CDOM	concentration_of_coloured_dissolved_organic_matter	0	400	1e ⁻⁹
VBSC	volumetric_scattering_function	0	0.1	m ⁻¹ sr ⁻¹
IRRADxxx*	downwelling_spectral_irradiance_in_sea_water_beamn ⁺	0	1000	uW cm ⁻² nm ⁻¹
HEAD	vehicle_heading	0	360	Degrees
UCUR	eastward_sea_water_velocity	-10	10	m s ⁻¹
VCUR	northward_sea_water_velocity	-10	10	m s ⁻¹
UCUR_GPS	eastward_surface_sea_water_velocity	-10	10	m s ⁻¹
VCUR_GPS	northward_surface_sea_water_velocity	-10	10	m s ⁻¹
PHASE	glider_trajectory_phase_code	0	6	1
PROFILE	glider_trajectory_profile_number	0	900000	1

\pm indicates a non-CF parameter. These parameters do not have associated standard names. Instead, *long_name* is listed.

* the codes are wave length dependant, different on each sensor. In total we have 7 generic wavelengths, i.e. ANFOG data contain the following parameters: IRRAD443, IRRAD490, IRRAD555, IRRAD670, IRRAD456, IRRAD 470 and IRRAD520. For instance for platform SL210, the four irradiance codes are: IRRAD443, IRRAD490, IRRAD555 and IRRAD670. The real wavelength, that is sometimes slightly different from the generic one (and differs from one sensor SN to another), is specified in the ‘comment’ attribute of the corresponding parameter.

+ n indicates the beam number, e.g. 1, 2, 3 or 4.

4.4 Spike test

The spike test is based on Argo Data Management (Argo, 2013) for temperature and salinity. A difference between sequential measurements, where one measurement is quite different than adjacent ones, is a spike in both size and gradient. The test does not consider the differences in depth, but assumes a sampling that adequately reproduces the temperature and salinity changes with depth. The algorithm is used on both the temperature and salinity profiles.

$$\text{Test value} = | V2 - (V3 + V1)/2 | - | (V3 - V1) / 2 |$$

where V2 is the measurement being tested as a spike, and V1 and V3 are the values above and below.

Temperature:

The V2 value is flagged (QC flag = 4) when

- the test value exceeds 6.0 degree C. for pressures less than 500 db or
- the test value exceeds 2.0 degree C. for pressures greater than or equal to 500 db

Salinity:

The V2 value is flagged (QC flag = 4) when

- the test value exceeds 0.9 PSU for pressures less than 500 db or
- the test value exceeds 0.3 PSU for pressures greater than or equal to 500 db

Presently, spikes in the other data types are manually flagged, although in the initial version of the ANFOG processing code, some automatic spike flagging had been implemented. In future, this may again be used.

4.5 Gradient test

This test is based on Argo Data Management (Argo, 2013). It fails when the difference between vertically adjacent measurements is too steep. The test does not consider the differences in depth, but assumes a sampling that adequately reproduces the temperature and salinity changes with depth. The algorithm is used on both the temperature and salinity profiles.

$$\text{Test value} = | V2 - (V3 + V1)/2 |$$

where V2 is the measurement being tested as a spike, and V1 and V3 are the values above and below.

Temperature: V2 value is flagged 4 when

- the test value exceeds 9.0 degree C for pressures less than 500 db or
- the test value exceeds 3.0 degree C. for pressures greater than or equal to 500 db

Salinity: V2 value is flagged 4 when

- the test value exceeds 1.5 PSU for pressures less than 500 db or
- the test value exceeds 0.5 PSU for pressures greater than or equal to 500 db

Presently, spikes in the other data types are manually flagged, although in the initial version of the ANFOG processing code, some automatic spike flagging using the gradient test had been implemented. In future, this may again be used.

4.6 Surface data

The surface (0 m to 0.5m depth) Chlorophyll-a fluorescence (CPHL), downwelling irradiance (IRRADxxx), coloured dissolved organic matter concentration (CDOM), volumetric backscatter (VBSC) and particulate backscatter coefficient (BBP) data are flagged 4 because these parameters are often noisy due to surface water interactions.

4.7 Descending IRRAD profiles

Radiometers are mounted on the Slocum gliders at an angle of -20⁰ to horizontal so that they are parallel to the ocean surface during glider ascent. Due to the cosine effect, downwelling irradiance measured on a flat plane decreases as a function of the cosine of the incoming light's average angle (Mobley, 1994; Berwald et.al, 1995; Kirk, 2011). Consequently, all descending upwelling irradiance data are flagged 4 due to incorrect orientation of the radiometer during glider descent.

5 Manual Corrections

Manual quality control is by subjective visual inspection of data values by an operator. To avoid delays, this is not mandatory before real-time distribution and is only performed in delayed mode.

The parameters that are visually checked and manually flagged are: PSAL, CNDC, TEMP, DOX1 (and thus DOX2), CPHL, CDOM, VBSC, BBP and IRRADxxx. The consistency in PSAL flags is also checked knowing that PSAL is calculated from CNDC and TEMP, as well as the consistency with DOX1 and DOX2 in case oxygen has been recomputed using TEMP, the temperature from the CTD, and in any case for DOX2, whose computation depends on density, i.e. PRES, TEMP and PSAL. Similarly, consistency for BBP is also checked as its computation is dependent on VBSC, PSAL and TEMP.

Examples of conditions where additional QC is applied:

- glider out of the water
- glider sitting in the seabed
- noise experienced due to bio-fouling or other reasons
- coarse outliers
- instrumental glitches

Apparently anomalous segments of data may be further investigated by considering environmental and geographical factors, as well as additional data, e.g. Sea-surface temperature satellite imagery.

6 QC Report

Each quality controlled NetCDF file (FV01) distributed in delayed mode is associated with a Quality Control report which contains information about the corrections applied to the data and their manual quality control. This report is not exhaustive and is distributed for information purposes only.

An associated FV00 NetCDF file which contains all the raw engineering parameters (not contained in the FV01 file) is also submitted to AODN, along with the raw files from the glider, a .kml Google Earth plot of the mission path/location and data time-series plots of the quality controlled data.

Bibliography

- Aanderaa (2007). *TD 218 Operating Manual Oxygen Optodes*.
- AODN Portal User Guide; Public Documents (2016). *Ocean Gliders - workflow* [online] Available at: <https://help.aodn.org.au/public-documents/imos/facilities/workflows/> [Accessed 15 Oct. 2018]
- Argo (2013). Argo User's Manual (Version 3.03).
- AUVAC (2018). *AUV System Spec Sheet* [online] Available at: http://auvac.org/uploads/configuration/Glider_structure.jpg [Accessed 15 Nov. 2018]
- Berwald, J., Stramski, D., Mobley, C.D. and Kiefer, D.A. (1995). Influences of Absorption and Scattering on Vertical Changes in the Average Cosine of the Underwater Light Field, *Limnology and Oceanography*, 40, 1347-1357.
- Bishop, C.M. (2008). *Sensor Dynamics of Autonomous Underwater Gliders*, Memorial University of Newfoundland, Newfoundland, USA.
- Boss, E., Pegau, W.S. (2001). Relationship of light scattering at an angle in the backwards direction to the backscattering coefficient, *Applied Optics*, 40 (30), 5503-5507.
- Cetinic, I., Toro-Farmer, G., Ragan, M., Oberg, C. and Jones, B.H., (2009). Calibration procedure for Slocum glider deployed optical instruments, *Optics Express*, 17 (18), 15420 – 15430.
- Farinato, R.S. and Rowell, R. L. (1976). New values of the light scattering depolarization and anisotropy of water, *J. Chem. Phys.*, 65, 593-595.
- Frajka-Williams, E., (2011). Determining Vertical Water Velocities from Seaglider, *Journal of Atmospheric and Oceanic Technology*, 28 (12), 1641-1656.
- Garau, B., Ruiz, S., Zhang, W., Pascual, A., Heslop, E., Kerfoot, J. and Tintoré, J. (2011). Thermal Lag Corrections on Slocum CTD Glider Data, *Journal of Atmospheric and Oceanic Technology*, 28, 1065-1071.
- Garcia, H.E. and Gordon, L.I. (1992). Oxygen Solubility in Seawater: Better Fitting Equations, *Limnology and Oceanography*, 37 (6), 1307-1312.
- Gregg, M.C. and Hess, W.C. (1985). Dynamic Response Calibration of Sea-Bird Temperature and Conductivity Probes, *Journal of Atmospheric and Oceanic Technology*, 2, 304-313.
- Horne, E.P.W. and Toole, J.M. (1980). Sensor Response Mismatches and Lag Correction Techniques for Temperature-Salinity Profilers. *Journal of Physical Oceanography*, 10, 1122-1130.
- Janzen, C. and Creed, E. (2011). Physical Oceanographic Data from Seaglider Trials in Stratified Coastal Waters Using a New Pumped Payload CTD, *OCEANS 2011 MTS/IEEE*, Kona, Hawaii, USA.
- Kerfoot, J., Glenn, S., Kohut, J., Schofield, O. and Roarty, H. (2006). *Correction for Sensor Mismatch and Thermal Lag effects in Non-pumped Conductivity-Temperature Sensors on the Slocum Coastal Electric Glider*, Ocean Science, Honolulu, Hawaii.
- Kirk, J.T.O. (2011). *Light and Photosynthesis in Aquatic Ecosystems*: Third Edition, Cambridge University Press.

- Lehaitre, M., Delauney, L. and Compere, C. (2008). Biofouling and underwater measurements. In: Babin, M., Roesler, C.S., Cullen, J.J. (eds) *Real-Time Coastal Observing Systems for Ecosystem Dynamics and Harmful Algal Bloom*, UNESCO Publishing , Paris, France, 463-494.
- Luek, R.G. and Picklo, J.J. (1990). Thermal Inertia of Conductivity Cells: Observations with a Sea-Bird Cell, *Journal of Atmospheric and Oceanic Technology*, 7, 756-768.
- Mantovanelli, A. and Thomson, P. (2016). Particle backscattering coefficient, ANFOG.
- Mobley, C.D. (1994). *Light and Water: Radiative Transfer in Natural Waters*, Academic Press.
- Morison, J., Andersen, N.L., D'Asaro, E. and Boyd, T. (1994). The correction for thermal-lag effects in Sea-Bird CTD data, *Journal of Atmospheric and Oceanic Technology*, 11, 1151-1164.
- Sea-Bird Electronics (2013). Seasoft V2: SBE Data Processing – CTD Data Processing and Plotting Software for Windows XP, Windows Vista, or Windows 7.
- Thierry, V., Gilbert, D., Kobayashi, T. and Schmid C. (2013). *Processing Argo OXYGEN data at the DAC level*.
- WETLabs (2013), Scattering Meter ECO BB-9, User's Guide, revision 22 August 2013.
- Woo, L.M., Gourcuff, C. and Hanson, C. (2018). *ANFOG Data Management User's Manual*, ANFOG.
- Zhang, X., Hu, L. and He, M. (2009). Scattering by pure seawater: Effect of salinity, *Optics Express*, 17 (7), 5698-5710.